Acta Cryst E CRYSTALLOGRAPHIC COMMUNICATIONS

ISSN 2056-9890

Synthesis, crystal structure and Hirshfeld surface analysis of bis(acetylacetonato-κ^2O,O')(2-amino-1-methyl-1*H*-benzimidazole-κN^3)copper(II)

Kyzlarkhan Siddikova,[a] Daminbek Ziyatov,[b]* Akmaljon Tojiboev,[c,d] Jamshid Ashurov,[e] Zukhra Kadirova[f] and Shahlo Daminova[b,f]

[a]Karshi Engineering Economics Institute, Mustakillik Avenue 225, Karshi 180100, Uzbekistan, [b]National University of Uzbekistan named after Mirzo Ulugbek, University Street 4, Tashkent 100174, Uzbekistan, [c]University of Geological Sciences, Olimlar Street 64, Tashkent 100125, Uzbekistan, [d]Namangan State University, Boburshox Street 161, Namangan 160107, Uzbekistan, [e]Institute of Bioorganic Chemistry, Academy of Sciences of Uzbekistan, Mirzo Ulugbek Street 83, Tashkent 100125, Uzbekistan, and [f]Uzbek-Japan Innovation Center of Youth, University Street 2B, Tashkent 100095, Uzbekistan. *Correspondence e-mail: ziatovdamin@gmail.com

Received 11 September 2024
Accepted 26 November 2024

Edited by B. Therrien, University of Neuchâtel, Switzerland

Keywords: benzimidazole; acetylacetone; copper complex; crystal structure; Hirshfeld surface analysis.

CCDC reference: 2405560

Supporting information: this article has supporting information at journals.iucr.org/e

The title compound, $[Cu(C_5H_7O_2)_2(C_8H_9N_3)]$, crystallizes in the orthorhombic space group *Pnma*. In the crystal structure, the Cu^{II} ion is coordinated by two acetylacetonate ligands and one 2-amino-1-methyl-1*H*-benzimidazole ligand. The crystal structure features intramolecular N—H···O and intermolecular N—H···O hydrogen bonds, which contribute to the overall cohesion of the crystal. Hirshfeld surface analysis and two-dimensional fingerprint plots were utilized to quantify the intermolecular interactions, revealing the relative contributions of H···H (61.1%), H···C/C···H (21.3%), and O···H/H···O (11.3%) contacts to the crystal packing.

1. Chemical context

Transition-metal complexes containing Schiff base ligands have garnered significant attention in recent years due to their promising catalytic activity in various reactions (Sheikhshoaie *et al.*, 2009; Hatefi *et al.*, 2010; Rezaeifard *et al.*, 2010). Benzimidazole derivatives have also attracted considerable interest due to their diverse biological and therapeutic activities, including antimicrobial properties against bacteria such as methicillin-resistant *staphylococcus aureus* (Gatadi *et al.*, 2019), *escherichia coli* (Mishra *et al.*, 2019), and *bacillus subtilis* (Song & Ma, 2016). The discovery of new benzimidazole compounds with novel antibacterial mechanisms is of paramount importance in addressing the growing threat of antibiotic resistance (Khalafi-Nezhad *et al.*, 2005). Recent research has focused on the synthesis and characterization of benzimidazole-based complexes with *d*-block metals (Jabborova *et al.*, 2024) and *f*-block metals (Ruzieva *et al.*, 2022), further expanding the potential applications of these compounds.

The coordination chemistry of rare-earth metals with β-diketonate ligands has been extensively studied due to their versatility and ease of use (Binnemans, 2005). β-Dicarbonyl compounds, known for their keto–enol tautomerism, are among the most widely investigated tautomeric systems (Tighadouini *et al.*, 2022; Harris, 2001). Metal acetylacetonates have found applications in diverse fields, including redox flow batteries (Suttil *et al.*, 2015) and as corrosion inhibitors for mild steel (Mahdavian & Attar, 2009). Notably, Cu^{II}, Ni^{II}, Co^{II}, and Zn^{II} complexes with acetylacetone ligands have demonstrated enhanced antimicrobial activity compared to

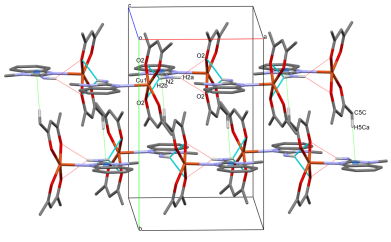

the free ligand (Raman *et al.*, 2003). In light of the potential biological significance of the title compound, [Cu($C_5H_7O_2$)$_2$($C_8H_9N_3$)], a detailed investigation of its crystal structure is presented.

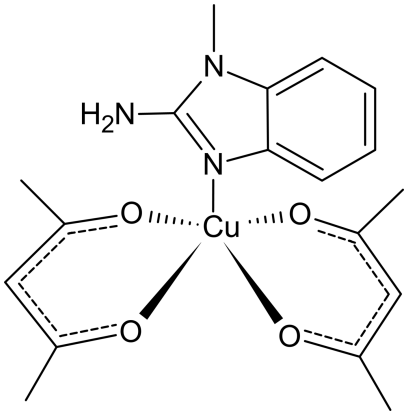

2. Structural commentary

The title compound, bis(acetylacetonato-κ^2O,O')(2-amino-1-methyl-1*H*-benzimidazole-κN^3)copper(II) (**I**), crystallizes in the orthorhombic space group *Pnma* (Fig. 1). The asymmetric unit consists of one molecule of 2-amino-1-methyl-1*H*-benzimidazole (**MAB**) and one acetylacetonate (**acac**) ligand, both coordinated to the central copper(II) ion. The Cu^{II} ion adopts a square-pyramidal coordination geometry (coordination number 5), with the equatorial plane defined by the oxygen atoms of two bidentate β-diketonate molecules [Cu1—O1 = 1.9378 (16) Å; Cu1—O2 = 1.9546 (16) Å; Table 1]. The observed elongation of the Cu—O bonds is attributed to the Jahn–Teller effect, a common phenomenon in copper-based complexes (Halcrow, 2013). The benzimidazole moiety is essentially planar and lies in the plane of symmetry (Fig. 2). The N1 atom of the benzimidazole ligand coordinates axially to the Cu^{II} ion with a bond distance of 2.196 (2) Å. The observed Cu—N1, Cu—O1, and Cu—O2 bond lengths are consistent with those reported for related Cu^{II} complexes (Geiger *et al.*, 2017; Wong *et al.*, 2009). The root-mean-square deviation of the equatorial plane (defined by O1, O2, Cu1, and their symmetry-related counterparts O1^{i} and O2^{i}) is 0.118 Å, with out-of-plane distances of 0.0596 (16) Å for O1 and 0.0582 (16) Å for O2. The largest deviation from the plane is observed for the Cu^{II} ion [0.2357 (4) Å], which is attributed to the presence of only one axial ligand (Fig. 1). The molecular structure of **I** exhibits intramolecular N—H···O hydrogen bonds (Table 2), which contribute to the stability of the individual molecules. These hydrogen bonds form a characteristic $S_1^1(6)$ graph-set motif (Etter *et al.*, 1990).

Table 1
Selected bond lengths (Å).

Cu1—O1^{i}	1.9378 (16)	Cu1—O2	1.9546 (16)
Cu1—O1	1.9378 (16)	Cu1—O2^{i}	1.9546 (16)
Cu1—N1	2.196 (2)		

Symmetry code: (i) $x, -y+\frac{1}{2}, z$.

Table 2
Hydrogen-bond geometry (Å, °).

*Cg*1 is the centroid of the N1/C2/N3/C3*A*/C7*A* ring.

D—H···*A*	*D*—H	H···*A*	*D*···*A*	*D*—H···*A*
N2—H2*A*···O2	0.86	2.44	3.077 (3)	131
N2—H2*B*···O2^{ii}	0.86	2.44	3.167 (3)	142
C5*B*—H5*BA*···*Cg*1^{iii}	0.96	2.74	3.682 (4)	166

Symmetry codes: (ii) $x-\frac{1}{2}, -y+\frac{1}{2}, -z+\frac{1}{2}$; (iii) $-x+1, y+\frac{1}{2}, -z+1$.

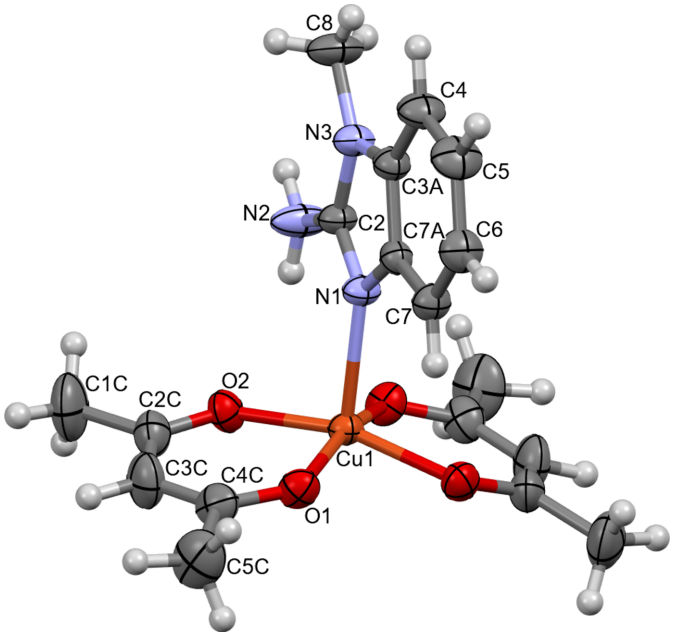

Figure 1
Molecular structure of the title compound. Displacement ellipsoids are drawn at the 30% probability level. The hydrogen atoms and symmetry-generated atoms are not labeled.

3. Supramolecular features

Intermolecular N—H···O hydrogen bonds play a crucial role in establishing the overall crystal packing. These inter-

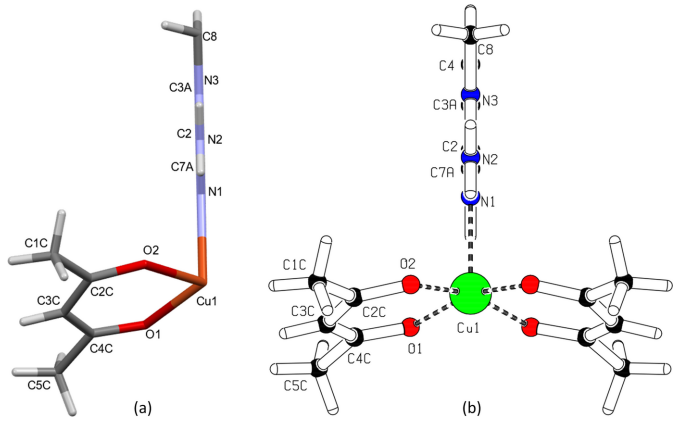

Figure 2
(*a*) The asymmetric unit in the crystal of **I**. (*b*) Emphasis on the benzimidazole planarity.

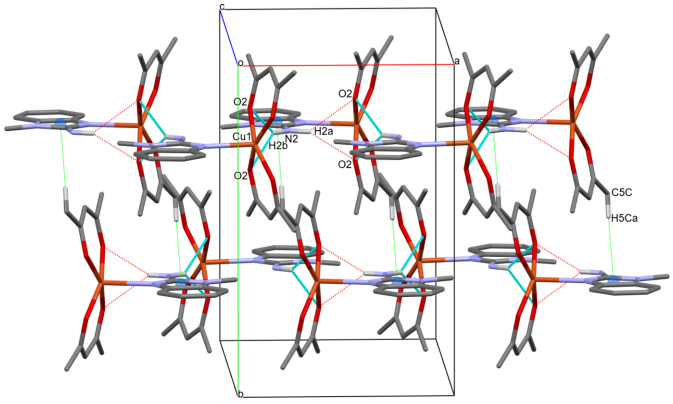

Figure 3
Crystal packing of **I** along the *c* axis. Intramolecular N—H···O hydrogen bonds are shown as red and intermolecular N—H···O hydrogen bonds as light-blue dashed lines. Dashed green lines denote C—H···*Cg*1 contacts. For clarity, H atoms not involved in these interactions have been omitted.

molecular interactions link the molecules into a zigzag chain running along the crystallographic a-axis direction, as depicted in Fig. 3. The graph-set descriptors for these chains are $C_1^1(6)$ and $R_2^1(4)$, further illustrating the connectivity of the hydrogen-bonded network.

The structure also features π-ring interactions between adjacent chains, which contribute to the overall cohesion of the crystal. These interactions involve C—H···π contacts, where the C5—H5*C* bond of one molecule interacts with the centroid (*Cg*1) of the N1/C2/N3/C3*A*/C7*A* ring of a neighbouring molecule. The distance between the hydrogen atom (H5*C*) and the ring centroid (*Cg*1) is 2.743 (16) Å, indicating a significant interaction.

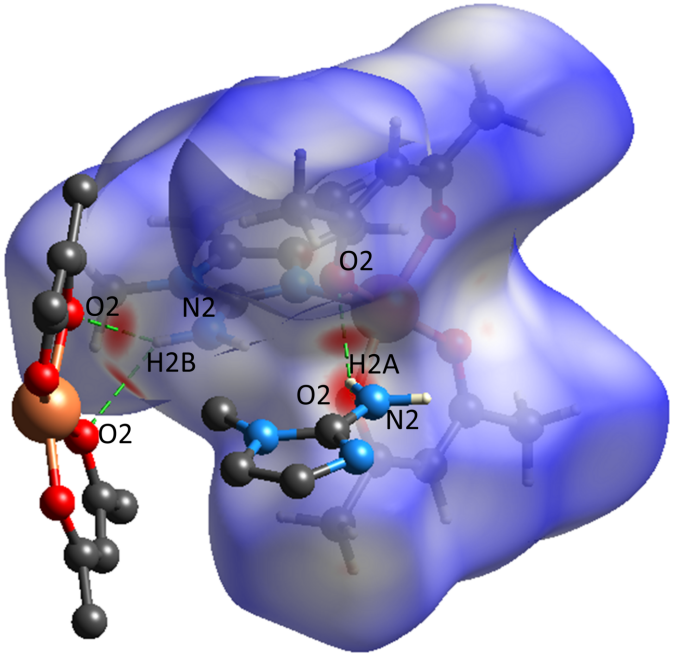

Figure 4
View of the three-dimensional Hirshfeld surface of **I** plotted over d_{norm}.

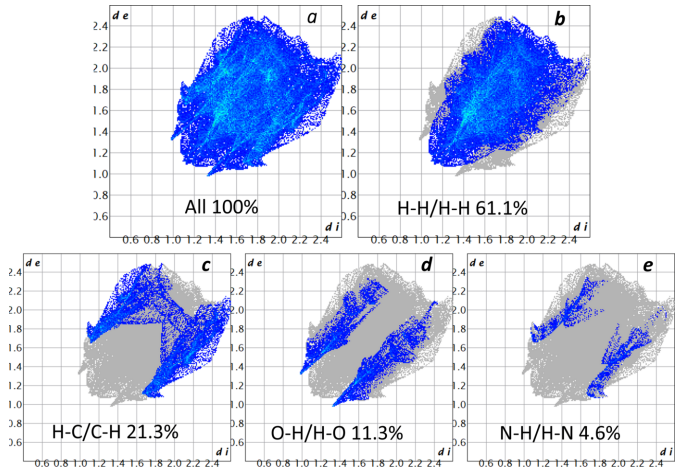

Figure 5
The full two-dimensional fingerprint plots for **I**, showing (*a*) all interactions and (*b*)–(*d*) delineated into separate interactions.

The combination of intramolecular and intermolecular hydrogen bonds, along with π-ring interactions, results in a robust three-dimensional supramolecular network in the crystal structure of **I**. These interactions not only contribute to the overall cohesion of the crystal but may also influence the physical and chemical properties of the compound.

4. Hirshfeld surface analysis

Hirshfeld surface analysis was conducted using *CrystalExplorer* 21.5 (Spackman *et al.*, 2021) to gain further insights into the intermolecular interactions in the crystal structure of **I**. The d_{norm} surface, shown in Fig. 4, is mapped over −0.2120 to −1.5316 arbitrary units (a.u.), with red, white, and blue regions representing contacts shorter, equal to, or longer than the sum of van der Waals radii, respectively(Venkatesan *et al.*, 2016).

The overall two-dimensional fingerprint plot (Fig. 5*a*) and its decomposed components illustrate the relative contributions of different intermolecular contacts to the Hirshfeld surface. As expected, H···H contacts (Fig. 5*b*) constitute the most significant contribution, accounting for 61.1% of the total Hirshfeld surface area. H···C/C···H contacts (Fig. 5*c*) comprise 21.3%, followed by O···H/H···O contacts (Fig. 5*d*) at 11.3%. The remaining contributions, including N···H/H···N (4.6%), Cu···C (1.0%), and C···C (0.7%), are relatively minor. These results highlight the dominance of van der Waals interactions in the crystal packing of **I**.

5. Database survey

A search of the Cambridge Structural Database (CSD, Version 5.45, November 2023; Groom *et al.*, 2016) revealed two related structures: bis(acetylacetonato-κ^2O,O')(2-amino-1-methyl-1*H*-benzimidazole-κN)oxidovanadium(IV) (Kadirova *et al.*, 2009; CSD refcode BOVMAB) and aqua-

(benzimidazole-*N*)bis(2,4-pentanedionato-*O*,*O*′)cobalt(II) (Lin & Feng, 2003; CSD refcode ESUZUN). In both cases, the benzimidazole ligand coordinates to the central metal ion through the sp^2 nitrogen atom (N3), as observed in **I**. However, the coordination geometries and overall structural features differ due to the presence of different metal centers and additional ligands in these related complexes.

6. Synthesis and crystallization

All reagents and solvents were of analytical grade and used as received. Elemental analysis was performed using a FlashSmart™ Elemental Analyzer. The Fourier-transform infrared (FT–IR) spectrum was recorded on a Spectrum Two N FT–IR Spectrometer at room temperature.

Solutions of 0.1 mmol (0.0261 g) of $CuCl_2{\cdot}6H_2O$ in ethanol (solution *A*), 0.2 mmol (0.0294 g) of 2-amino-1-methyl-1*H*-benzimidazole (MAB) in ethanol (solution *B*), and 0.2 mmol (0.0205 mL, ρ = 0.975 g mL^{-1}) of acetylacetone (solution *C*) were prepared. Solution *B* was added dropwise to solution *A* with stirring at room temperature for 30 minutes; no immediate changes being observed. Subsequently, solution *C* was added dropwise to the mixture, followed by stirring for 12 h. The resulting solution was then allowed to stand undisturbed at room temperature. Blue–green crystals formed over several days, which were then filtered, washed with ethanol, and recrystallized from dimethyl sulfoxide to yield light-green crystals suitable for X-ray diffraction analysis.

Elemental analysis: Calculated for $C_{18}H_{23}CuN_3O_4$: C, 52.88; H, 5.67; N, 10.28%. Found: C, 53.06; H, 5.33; N, 10.59%.

FT–IR (cm^{-1}): 3448*s*, 3341*s*, 3054*s*, 2935*m*, 1654*s*, 1612*s*, 1584*s*, 1551*s*, 1522*s*, 1499*s*, 1399*s*, 1319*s*, 1289*s*, 1200*m*, 1108*s*, 1089*m*, 1018*s*, 934*s*, 894*m*, 787*s*, 746*s*, 674*m*, 657*s*, 587*s*, 566*m*, 429*m*.

7. Refinement

Crystal data, data collection, and structure refinement details are summarized in Table 3. Hydrogen atoms bonded to carbon were positioned geometrically (C—H = 0.93 Å for aromatic, 0.96 Å for methyl, and 0.97 Å for methylene) and refined using a riding model, with U_{iso}(H) = 1.5U_{eq}(C) for methyl hydrogens and 1.2U_{eq}(C) for all others. The amine group (–NH_2) hydrogen atoms were located in a difference-Fourier map and refined with an N—H distance restraint of 0.86 (2) Å and U_{iso}(H) = 1.5U_{eq}(N).

Table 3
Experimental details.

Crystal data	
Chemical formula	$[Cu(C_5H_7O_2)_2(C_8H_9N_3)]$
M_r	408.93
Crystal system, space group	Orthorhombic, *Pnma*
Temperature (K)	298
a, *b*, *c* (Å)	9.0322 (2), 13.9740 (3), 16.0004 (4)
V (Å^3)	2019.51 (8)
Z	4
Radiation type	Cu *Kα*
μ (mm^{-1})	1.70
Crystal size (mm)	0.3 × 0.24 × 0.18
Data collection	
Diffractometer	XtaLAB Synergy, Single source at home/near, HyPix3000
Absorption correction	Multi-scan (*CrysAlis PRO*; Rigaku OD, 2020)
T_{min}, T_{max}	0.517, 1.000
No. of measured, independent and observed [$I \geq 2\sigma(I)$] reflections	19729, 2050, 1693
R_{int}	0.066
(sin $\theta/\lambda)_{max}$ (Å^{-1})	0.615
Refinement	
$R[F^2 > 2\sigma(F^2)]$, $wR(F^2)$, *S*	0.036, 0.109, 1.04
No. of reflections	2050
No. of parameters	146
H-atom treatment	H atoms treated by a mixture of independent and constrained refinement
$\Delta\rho_{max}$, $\Delta\rho_{min}$ (e Å^{-3})	0.27, −0.34

Computer programs: *CrysAlis PRO* (Rigaku OD, 2020), *SHELXT2014/5* (Sheldrick, 2015), *OLEX2.refine* (Bourhis *et al.*, 2015) and *OLEX2* (Dolomanov *et al.*, 2009).

Acknowledgements

The authors acknowledge support from the MIRAI FUND (JICA) and technical equipment support provided by the Institute of Bioorganic Chemistry of Academy Sciences of Uzbekistan.

References

Binnemans, K. (2005). *Handbook on the Physics, Chemistry of Rare Earths*, vol. 35, ch. 225, pp 107–185. Amsterdam: Elsevier.
Bourhis, L. J., Dolomanov, O. V., Gildea, R. J., Howard, J. A. K. & Puschmann, H. (2015). *Acta Cryst.* A**71**, 59–75.
Dolomanov, O. V., Bourhis, L. J., Gildea, R. J., Howard, J. A. K. & Puschmann, H. (2009). *J. Appl. Cryst.* **42**, 339–341.
Etter, M. C., MacDonald, J. C. & Bernstein, J. (1990). *Acta Cryst.* B**46**, 256–262.
Gatadi, S., Madhavi, Y. V., Chopra, S. & Nanduri, S. (2019). *Bioorg. Chem.* **92**, 364–377.
Geiger, D. K., DeStefano, M. R. & Lewis, R. A. (2017). *Acta Cryst.* E**73**, 1616–1621.
Groom, C. R., Bruno, I. J., Lightfoot, M. P. & Ward, S. C. (2016). *Acta Cryst.* B**72**, 171–179.
Halcrow, M. A. (2013). *Chem. Soc. Rev.* **42**, 1784–1795.
Harris, T. M. (2001). 2,4-Pentanedione. In *Encyclopedia of Reagents for Organic Synthesis.* Chichester: Wiley.
Hatefi, M., Moghadam, M., Mirkhani, V. & Sheikhshoaei, I. (2010). *Polyhedron*, **29**, 2953–2958.
Jabborova, K., Ashurov, J., Tojiboev, A. & Daminova, S. (2024). *Acta Cryst.* E**80**, 751–754.
Kadirova, Z. C., Rahmonova, D. S., Talipov, S. A., Ashurov, J. M. & Parpiev, N. A. (2009). *Acta Cryst.* E**65**, m819.
Khalafi-Nezhad, A., Soltani Rad, M. N., Mohabatkar, H., Asrari, Z. & Hemmateenejad, B. (2005). *Bioorg. Med. Chem.* **13**, 1931–1938.
Lin, H. & Feng, Y. L. (2003). *Z. Kristallogr. New Cryst. Struct.* **218**, 533–534.
Mahdavian, M. & Attar, M. M. (2009). *Corros. Sci.* **51**, 409–414.
Mishra, V. R., Ghanavatkar, C. W., Mali, S. N., Qureshi, S. I., Chaudhari, H. K. & Sekar, N. (2019). *Comput. Biol. Chem.* **78**, 330–337.

Raman, N., Muthuraj, V., Ravichandran, S. & Kulandaisamy, A. (2003). *J. Chem. Sci.* **115**, 161–167.

Rezaeifard, A., Sheikhshoaie, I., Monadi, N. & Stoeckli–Evans, H. (2010). *Eur. J. Inorg. Chem.* pp. 799–806.

Rigaku OD (2020). *CrysAlis PRO*. Rigaku Oxford Diffraction, Yarnton, England.

Ruzieva, B., Kunafiev, R., Kadirova, Z. & Daminova, S. (2022). *Acta Cryst.* E**78**, 647–651.

Sheikhshoaie, I., Rezaeifard, A., Monadi, N. & Kaafi, S. (2009). *Polyhedron*, **28**, 733–738.

Sheldrick, G. M. (2015). *Acta Cryst*. A**71**, 3–8.

Song, D. & Ma, S. (2016). *ChemMedChem*, **11**, 646–659.

Spackman, P. R., Turner, M. J., McKinnon, J. J., Wolff, S. K., Grimwood, D. J., Jayatilaka, D. & Spackman, M. A. (2021). *J. Appl. Cryst.* **54**, 1006–1011.

Suttil, J. A., Kucharyson, J. F., Escalante-Garcia, I. L., Cabrera, P. J., James, B. R., Savinell, R. F., Sanford, M. S. & Thompson, L. T. (2015). *J. Mater. Chem. A*, **3**, 7929–7938.

Tighadouini, S., Roby, O., Mortada, S., Lakbaibi, Z., Radi, S., Al-Ali, A., Faouzi, M. E. A., Ferbinteanu, M., Garcia, Y., Al-Zaqri, N., Zarrouk, A. & Warad, I. (2022). *J. Mol. Struct.* **1247**, 131308.

Venkatesan, P., Thamotharan, S., Ilangovan, A., Liang, H. & Sundius, T. (2016). *Spectrochim. Acta A Mol. Biomol. Spectrosc.* **153**, 625–636.

Wong, Y. S., Ng, C. H. & Ng, S. W. (2009). *Acta Cryst.* E**65**, m934.

supporting information

Acta Cryst. (2025). E**81**, 1-5 [https://doi.org/10.1107/S2056989024011538]

Synthesis, crystal structure and Hirshfeld surface analysis of bis(acetylacetonato-κ^2O,O')(2-amino-1-methyl-1*H*-benzimidazole-κN^3)copper(II)

Kyzlarkhan Siddikova, Daminbek Ziyatov, Akmaljon Tojiboev, Jamshid Ashurov, Zukhra Kadirova and Shahlo Daminova

Computing details

Bis(acetylacetonato-κ^2O,O')(2-amino-1-methyl-1*H*-\ benzimidazole-κN^3)copper(II)

Crystal data

$[Cu(C_5H_7O_2)_2(C_8H_9N_3)]$
M_r = 408.93
Orthorhombic, *Pnma*
a = 9.0322 (2) Å
b = 13.9740 (3) Å
c = 16.0004 (4) Å
V = 2019.51 (8) Å^3
Z = 4
F(000) = 846.676
D_x = 1.345 Mg m^{-3}
Cu *Kα* radiation, λ = 1.54184 Å
Cell parameters from 5665 reflections
θ = 2.8–69.5°
μ = 1.70 mm^{-1}
T = 298 K
Block, clear light green
0.3 × 0.24 × 0.18 mm

Data collection

XtaLAB Synergy, Single source at home/near, HyPix3000 diffractometer
Detector resolution: 10.0000 pixels mm^{-1}
ω scans
Absorption correction: multi-scan (CrysAlisPro; Rigaku OD, 2020)
T_{min} = 0.517, T_{max} = 1.000
19729 measured reflections
2050 independent reflections
1693 reflections with $I \geq 2\sigma(I)$
R_{int} = 0.066
θ_{max} = 71.5°, θ_{min} = 4.2°
h = −11→10
k = −17→17
l = −19→19

Refinement

Refinement on F^2
Least-squares matrix: full
$R[F^2 > 2\sigma(F^2)]$ = 0.036
$wR(F^2)$ = 0.109
S = 1.04
2050 reflections
146 parameters
0 restraints
Hydrogen site location: mixed
H atoms treated by a mixture of independent and constrained refinement
$w = 1/[\sigma^2(F_o^2) + (0.0585P)^2 + 0.436P]$ where $P = (F_o^2 + 2F_c^2)/3$
$(\Delta/\sigma)_{max}$ = 0.001
$\Delta\rho_{max}$ = 0.27 e Å^{-3}
$\Delta\rho_{min}$ = −0.33 e Å^{-3}
Extinction correction: SHELXL2016/6 (Sheldrick 2015), $Fc^*=kFc[1+0.001xFc^2\lambda^3/\sin(2\theta)]^{-1/4}$
Extinction coefficient: 0.00034 (14)

Special details

Geometry. All esds (except the esd in the dihedral angle between two l.s. planes) are estimated using the full covariance matrix. The cell esds are taken into account individually in the estimation of esds in distances, angles and torsion angles; correlations between esds in cell parameters are only used when they are defined by crystal symmetry. An approximate (isotropic) treatment of cell esds is used for estimating esds involving l.s. planes.

Fractional atomic coordinates and isotropic or equivalent isotropic displacement parameters (Å²)

	x	*y*	*z*	U_{iso}*/U_{eq}
Cu1	0.58425 (4)	0.250000	0.42118 (3)	0.04582 (19)
O1	0.66063 (18)	0.34444 (12)	0.49868 (10)	0.0623 (4)
N1	0.3473 (2)	0.250000	0.45198 (15)	0.0466 (6)
O2	0.56911 (18)	0.34360 (12)	0.33081 (10)	0.0615 (4)
N2	0.2624 (3)	0.250000	0.31270 (17)	0.0819 (10)
H2A	0.350932	0.250000	0.292910	0.098*
H2B	0.187784	0.250000	0.279310	0.098*
C3	0.2406 (3)	0.250000	0.39601 (18)	0.0492 (7)
C7A	0.2752 (3)	0.250000	0.52873 (17)	0.0440 (6)
C8	−0.0378 (5)	0.250000	0.3850 (3)	0.0828 (14)
C3A	0.1225 (3)	0.250000	0.5159 (2)	0.0507 (7)
C4B	0.6857 (3)	0.43114 (19)	0.48236 (19)	0.0713 (7)
C5	0.0806 (4)	0.250000	0.6613 (3)	0.0798 (12)
H5	0.017475	0.250000	0.707242	0.096*
C2B	0.5995 (3)	0.4322 (2)	0.33641 (19)	0.0724 (7)
N3	0.1028 (3)	0.250000	0.43016 (16)	0.0534 (7)
C3B	0.6587 (4)	0.4754 (2)	0.4067 (2)	0.0907 (10)
H3B	0.682585	0.539925	0.402560	0.109*
C4	0.0195 (4)	0.250000	0.5807 (2)	0.0701 (10)
H4	−0.082124	0.250000	0.571234	0.105*
C5B	0.7560 (5)	0.4878 (3)	0.5527 (2)	0.1149 (14)
H5BA	0.760146	0.554218	0.537488	0.172*
H5BB	0.854430	0.464517	0.562579	0.172*
H5BC	0.697939	0.480611	0.602556	0.172*
C6	0.2322 (4)	0.250000	0.6747 (2)	0.0671 (9)
H6	0.267621	0.250000	0.729239	0.080*
C7	0.3321 (4)	0.250000	0.6096 (2)	0.0550 (7)
H7	0.433621	0.250000	0.619289	0.066*
C1B	0.5684 (6)	0.4893 (2)	0.2591 (2)	0.1206 (15)
H1BA	0.574813	0.556314	0.271846	0.181*
H1BB	0.470795	0.474659	0.239196	0.181*
H1BC	0.639781	0.473498	0.216864	0.181*
H8A	−0.049 (6)	0.199 (3)	0.353 (3)	0.19 (2)*
H8B	−0.100 (8)	0.250000	0.420 (4)	0.14 (3)*

Atomic displacement parameters (Å²)

	U^{11}	U^{22}	U^{33}	U^{12}	U^{13}	U^{23}
Cu1	0.0410 (3)	0.0525 (3)	0.0439 (3)	0.000	0.00055 (16)	0.000

O1	0.0659 (10)	0.0630 (10)	0.0580 (9)	0.0026 (8)	−0.0107 (7)	−0.0074 (8)
N1	0.0368 (12)	0.0605 (14)	0.0426 (12)	0.000	0.0026 (10)	0.000
O2	0.0728 (11)	0.0612 (10)	0.0505 (9)	−0.0109 (7)	0.0010 (7)	0.0085 (7)
N2	0.0433 (16)	0.160 (3)	0.0422 (14)	0.000	−0.0035 (12)	0.000
C3	0.0360 (14)	0.0645 (18)	0.0471 (15)	0.000	0.0009 (12)	0.000
C7A	0.0464 (15)	0.0420 (13)	0.0435 (14)	0.000	0.0033 (12)	0.000
C8	0.041 (2)	0.137 (5)	0.070 (3)	0.000	−0.0072 (19)	0.000
C3A	0.0441 (15)	0.0556 (17)	0.0524 (17)	0.000	0.0055 (13)	0.000
C4B	0.0746 (17)	0.0566 (14)	0.0828 (18)	0.0047 (12)	−0.0081 (14)	−0.0184 (13)
C5	0.071 (3)	0.114 (3)	0.055 (2)	0.000	0.0223 (17)	0.000
C2B	0.0847 (19)	0.0593 (15)	0.0731 (17)	−0.0010 (13)	0.0100 (14)	0.0128 (13)
N3	0.0374 (13)	0.0733 (18)	0.0494 (14)	0.000	−0.0018 (10)	0.000
C3B	0.129 (3)	0.0480 (14)	0.095 (2)	−0.0085 (16)	−0.009 (2)	−0.0014 (14)
C4	0.050 (2)	0.097 (3)	0.064 (2)	0.000	0.0117 (15)	0.000
C5B	0.148 (4)	0.078 (2)	0.119 (3)	0.000 (2)	−0.038 (3)	−0.039 (2)
C6	0.073 (2)	0.083 (2)	0.0449 (16)	0.000	0.0051 (15)	0.000
C7	0.0554 (19)	0.0618 (19)	0.0477 (16)	0.000	−0.0022 (14)	0.000
C1B	0.187 (4)	0.083 (2)	0.092 (3)	−0.013 (2)	−0.004 (2)	0.036 (2)

Geometric parameters (Å, º)

Cu1—O1^{i}	1.9378 (16)	C3A—C4	1.393 (5)
Cu1—O1	1.9378 (16)	C4B—C3B	1.381 (4)
Cu1—N1	2.196 (2)	C4B—C5B	1.516 (4)
Cu1—O2	1.9546 (16)	C5—H5	0.9300
Cu1—O2^{i}	1.9546 (16)	C5—C4	1.404 (6)
O1—C4B	1.260 (3)	C5—C6	1.385 (5)
N1—C3	1.316 (4)	C2B—C3B	1.383 (4)
N1—C7A	1.390 (3)	C2B—C1B	1.498 (4)
O2—C2B	1.272 (3)	C3B—H3B	0.9300
N2—H2A	0.8600	C4—H4	0.9300
N2—H2B	0.8600	C5B—H5BA	0.9600
N2—C3	1.348 (4)	C5B—H5BB	0.9600
C3—N3	1.360 (4)	C5B—H5BC	0.9600
C7A—C3A	1.395 (4)	C6—H6	0.9300
C7A—C7	1.392 (4)	C6—C7	1.378 (5)
C8—N3	1.461 (5)	C7—H7	0.9300
C8—H8A	0.89 (5)	C1B—H1BA	0.9600
C8—H8A^{i}	0.89 (5)	C1B—H1BB	0.9600
C8—H8B	0.79 (7)	C1B—H1BC	0.9600
C3A—N3	1.383 (4)		

O1^{i}—Cu1—O1	85.85 (10)	C3B—C4B—C5B	119.4 (3)
O1—Cu1—N1	101.73 (7)	C4—C5—H5	119.0
O1^{i}—Cu1—N1	101.73 (7)	C6—C5—H5	119.0
O1—Cu1—O2	92.44 (7)	C6—C5—C4	122.0 (3)
O1^{i}—Cu1—O2^{i}	92.44 (7)	O2—C2B—C3B	124.4 (3)
O1—Cu1—O2^{i}	162.56 (7)	O2—C2B—C1B	114.8 (3)

O1^{i}—Cu1—O2	162.56 (7)	C3B—C2B—C1B	120.8 (3)
O2—Cu1—N1	95.61 (7)	C3—N3—C8	126.6 (3)
O2^{i}—Cu1—N1	95.61 (7)	C3—N3—C3A	106.3 (2)
O2^{i}—Cu1—O2	84.01 (10)	C3A—N3—C8	127.1 (3)
C4B—O1—Cu1	125.89 (18)	C4B—C3B—C2B	125.9 (3)
C3—N1—Cu1	124.14 (19)	C4B—C3B—H3B	117.1
C3—N1—C7A	105.0 (2)	C2B—C3B—H3B	117.1
C7A—N1—Cu1	130.90 (19)	C3A—C4—C5	114.9 (3)
C2B—O2—Cu1	125.76 (18)	C3A—C4—H4	122.5
H2A—N2—H2B	120.0	C5—C4—H4	122.5
C3—N2—H2A	120.0	C4B—C5B—H5BA	109.5
C3—N2—H2B	120.0	C4B—C5B—H5BB	109.5
N1—C3—N2	124.5 (3)	C4B—C5B—H5BC	109.5
N1—C3—N3	113.4 (3)	H5BA—C5B—H5BB	109.5
N2—C3—N3	122.1 (3)	H5BA—C5B—H5BC	109.5
N1—C7A—C3A	109.5 (3)	H5BB—C5B—H5BC	109.5
N1—C7A—C7	130.4 (3)	C5—C6—H6	119.0
C7—C7A—C3A	120.1 (3)	C7—C6—C5	122.1 (3)
N3—C8—H8A^{i}	112 (3)	C7—C6—H6	119.0
N3—C8—H8A	112 (3)	C7A—C7—H7	121.3
N3—C8—H8B	105 (5)	C6—C7—C7A	117.4 (3)
H8A—C8—H8A^{i}	108 (6)	C6—C7—H7	121.3
H8A—C8—H8B	109 (4)	C2B—C1B—H1BA	109.5
H8B—C8—H8A^{i}	109 (4)	C2B—C1B—H1BB	109.5
N3—C3A—C7A	105.9 (2)	C2B—C1B—H1BC	109.5
N3—C3A—C4	130.7 (3)	H1BA—C1B—H1BB	109.5
C4—C3A—C7A	123.5 (3)	H1BA—C1B—H1BC	109.5
O1—C4B—C3B	125.5 (3)	H1BB—C1B—H1BC	109.5
O1—C4B—C5B	115.1 (3)		

Cu1—O1—C4B—C3B	2.1 (4)	C3—N1—C7A—C7	180.000 (1)
Cu1—O1—C4B—C5B	−175.7 (2)	C7A—N1—C3—N2	180.000 (1)
Cu1—N1—C3—N2	0.000 (1)	C7A—N1—C3—N3	0.000 (1)
Cu1—N1—C3—N3	180.000 (1)	C7A—C3A—N3—C3	0.000 (1)
Cu1—N1—C7A—C3A	180.000 (1)	C7A—C3A—N3—C8	180.000 (1)
Cu1—N1—C7A—C7	0.000 (1)	C7A—C3A—C4—C5	0.000 (1)
Cu1—O2—C2B—C3B	4.8 (4)	C3A—C7A—C7—C6	0.000 (1)
Cu1—O2—C2B—C1B	−176.0 (2)	C5—C6—C7—C7A	0.000 (1)
O1—C4B—C3B—C2B	0.3 (6)	N3—C3A—C4—C5	180.000 (1)
N1—C3—N3—C8	180.000 (1)	C4—C3A—N3—C3	180.000 (1)
N1—C3—N3—C3A	0.000 (1)	C4—C3A—N3—C8	0.000 (1)
N1—C7A—C3A—N3	0.000 (1)	C4—C5—C6—C7	0.000 (1)
N1—C7A—C3A—C4	180.000 (1)	C5B—C4B—C3B—C2B	178.0 (4)
N1—C7A—C7—C6	180.000 (1)	C6—C5—C4—C3A	0.000 (1)
O2—C2B—C3B—C4B	−4.1 (6)	C7—C7A—C3A—N3	180.000 (1)
N2—C3—N3—C8	0.000 (1)	C7—C7A—C3A—C4	0.000 (1)

N2—C3—N3—C3A	180.000 (1)	C1B—C2B—C3B—C4B	176.9 (4)
C3—N1—C7A—C3A	0.000 (1)		

Symmetry code: (i) *x*, −*y*+1/2, *z*.

Hydrogen-bond geometry (Å, º)

*Cg*1 is the centroid of the N1/C2/N3/C3*A*/C7*A* ring.

D—H···*A*	*D*—H	H···*A*	*D*···*A*	*D*—H···*A*
N2—H2*A*···O2	0.86	2.44	3.077 (3)	131
N2—H2*B*···O2^{ii}	0.86	2.44	3.167 (3)	142
C5*B*—H5*BA*···*Cg*1^{iii}	0.96	2.74	3.682 (4)	166

Symmetry codes: (ii) *x*−1/2, −*y*+1/2, −*z*+1/2; (iii) −*x*+1, *y*+1/2, −*z*+1.